TECHNICAL RESEARCH REPORT

Institute for Systems Research

An Improved Model for the Dynamics of Spur Gear Systems with Backlash Consideration

by T.K. Shing, L.W. Tsai and P.S. Krishnaprasad

The Institute for Systems Research is supported by the National Science Foundation Engineering Research Center Program (NSFD CD 8803012), Industry and the University

TR 93-28

An Improved Model for the Dynamics of Spur Gear Systems with Backlash Consideration

T. K. Shing, Graduate Research Assistant

L. W. Tsai, Professor

Mechanical Engineering Department

and

Institute for Systems Research

P. S. Krishnaprasad, Professor

Electrical Engineering Department

and

Institute for Systems Research

University of Maryland

College Park, MD 20742

Abstract

An improved model which accounts for backlash effects is proposed for the dynamics of spur gear systems. This dynamic model is mainly developed for the purpose of real time control. The complicated variation of the meshing stiffness as a function of contact point along the line of action is studied. Then the mean value is used as the stiffness constant in the improved model. Two simulations, free vibration and constant load operation, are performed to illustrate the effects of backlash on gear dynamics. Also given are comparisons of the simulation results with that of the Yang and Sun's model. This model is judged to be more realistic which can be used in real time control to achieve high precision.

Nomenclature

A	point of intersection between the line of action and the base circle of gear 1
B	point of intersection between the line of action and the base circle of gear 2
C	point of intersection between the line of action and the addendum circle of gear 2
CF	=ED=p_b region of double-tooth contact
D	point of intersection between the line of action and the addendum circle of gear 1
E	Young's modulus of elasticity
F_n	normal contact force
I_j	second moment of inertia of gear j about its center of rotation
M	point of contact along line of action
O_j	center of gear j
P	pitch point
c	damping coefficient in a gear mesh
d	damping factor used in Yang and Sun's model
e	coefficient of restitution
f	face width
h_{aj}	radial distance measured from the dedendum circle to the addendum circle of gear j
h_{bj}	radial distance measured from the dedendum circle to the base circle of gear j
h_{cj}	radial distance measured from the dedendum circle to the meshing point of gear j
k	mesh stiffness constant
k_{ij}	spring constant of the jth tooth on gear i
l	length of AB
p_b	base pitch

r_{aj} radius of the addendum circle on gear j

r_{bj} radius of the base circle on gear j

r_{dj} radius of the dedendum circle on gear j

t_{aj} tooth thickness of gear j measured along the addendum circle

t_{bj} tooth thickness of gear j measured along the base circle

t_p tooth thickness at the pitch circle

δ_{bn} deflection due to bending caused by $F_n \sin\phi$

δ_{bp} deflection due to bending caused by $F_n \cos\phi$

δ_f deflection due to the flexibility of gear tooth foundation

δ_h Hertzian deflection due to the compression between gear teeth

δ_s deflection due to shear

ϕ pressure angle = 20 degree

ν Poisson's ratio

ϑ_j rotation angle of gear j measured from O_jC

α_{ij} rotation angle of the jth tooth on gear i measured from O_iA

θ_j angular displacement of gear j

ξ_j applied torque on gear j

1 Introduction

Gear trains are commonly used in robot manipulators and other kind of servomechanisms to amplify actuator torque and also to transmit power from one shaft to another. However, the backlash between meshing gear teeth can cause impact, reduce system stability, generate noise and undesired vibrations. The uncertainty caused by backlash will also decrease the repeatability and accuracy of a geared servomechanism. With the increasing demand of high precision, accurate dynamic modeling and control of geared servomechanisms become very important. Hence the effects of backlash, one of the main nonlinearities in a geared system, on the dynamics of a geared mechanism are studied in this paper.

The dynamics of spur gear systems has been investigated by numerous researchers (Remmers, 1971; Tobe and Takatsu, 1973; Rebbechi and Crisp, 1981; Ozguven and Houser, 1988; Comparin and Singh, 1989; Kahraman and Singh, 1989). A literature survey reveals that little effort has been made on the understanding of the effects of gear backlash and/or clearance on the dynamics of mechanical systems. Hunt and Crossley (1975), Herbert and McWhannell (1977), and Lee and Wang (1983) contributed to the understanding of the effects of impact and damping coefficient

estimation on the dynamics of intermittent motion mechanisms. Goodman (1963) proposed a method of calculating the dynamic effects caused by backlash in a mechanism. Dubowsky and Freudenstein (1971) created a rectilinear dynamic model, called the "Impact Pair," for mechanical systems with clearance. By extending Dubowsky and Freudenstein's model, Azar and Crossley (1977) investigated the dynamic behavior of a spur gear system with backlash using both computer simulations and experimental verification. Yang and Sun (1985) developed a circular model which is different from the rectilinear gear model introduced by Azar and Crossley for spur gear system with backlash. They also proposed an analytic method to estimate the stiffness constant and damping factor in two meshing gears.

The above mentioned studies on backlash had concentrated on the models of the instantaneous impact phenomena of a simple gear pair of such complexity that the models are not suitabel for the purpose of control. Hence, it is the objective of this study to establish a simplified dynamic model for real time control. To build an accurate dynamical model, parameters used in the model need to be estimated correctly. In a gear model, the meshing stiffness constant is difficult to estimate since it involves a very complicated phenomenon. The subject has been studied extensively by several researchers (Timoshenko and Baud, 1926; Nakada and Utagawa, 1956; O'Donnel, 1960; Matsuz et al., 1969; Elkholy, 1985; Tavakoli and Houser, 1986). Yang and Sun (1985) proposed a method to estimate the stiffness. However, in the Yang and Sun model, only the deflection due to Hertzian stress was considered, while all the other effects such as bending moment, shear stress, etc. were neglected. In this paper, it will be shown that the deflection due to Hertzian stress only constitutes to a small fraction of the overall deflection. Hence, the accuracy of Yang and Sun's model becomes questionable. It will also be shown that a mean-value stiffness constant can be used to accurately predict the dynamics of a geared system with clearance. We expect that this simplified model can be used for real-time control to improve the accuracy of a geared servomechanism.

2 Dynamic Model with Backlash Consideration

The basic structure of a single degree-of-freedom (DOF) gear pair is shown in Figure 1. The shafts of the two gears are assumed to be rigid and the only compliance considered in this model is the compliance of gear teeth. The mesh compliance, which will be examined later, consists of the effects of bending moment, shear stress, foundation inclination, and Hertzian contact compression

on a gear tooth. To make the model more realistic, backlash effects between two meshing gears will be considered. Backlash, which causes discontinuous phenomena and impact effects on dynamics, brings one uncertainty to the dynamic model of a single DOF system.

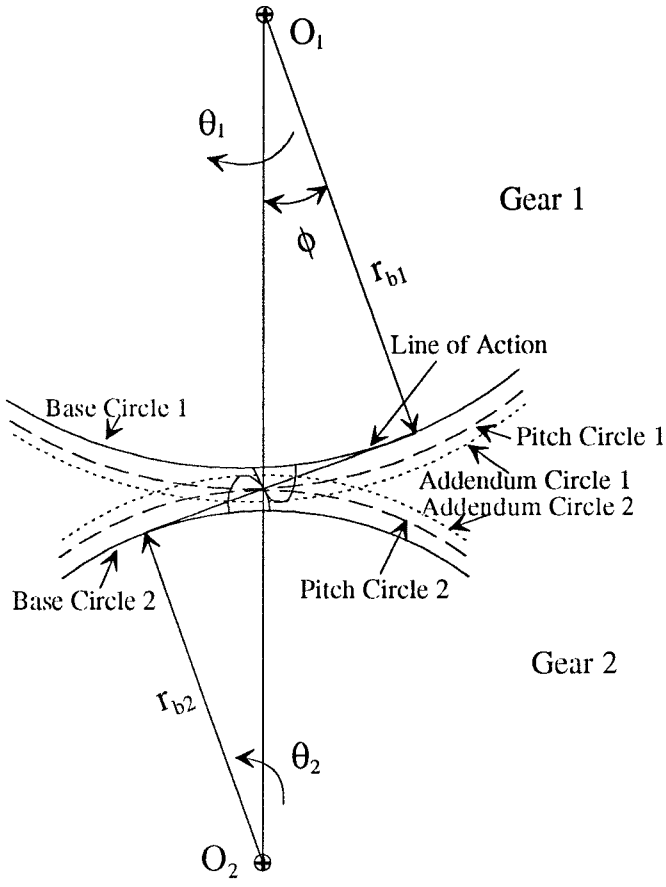

Figure 1: A gear pair in mesh

For convenience, some symbols and definitions will be made first. Backlash, b, will be defined as the clearance measured along the line of action of a gear pair as shown in Figure 2, Note that this definition of backlash is a little different from the definition found in some textbooks (Martin, 1982). But the difference is negligible. We define θ_1 and ξ_1 to be positive in the clockwise direction, and θ_2 and ξ_2 to be positive in the counterclockwise direction. The neutral position of a gear pair is defined as the position where the centerline of a tooth in the drive gear 1 and the center of a tooth space on the driven gear 2 are both coincident with the centerline of the two gear centers. The approach portion is the part from the first point of contact to the pitch point on the line of action and the recess portion is the part from the pitch point to the last point of contact. Due to backlash, there

are two kinds of contact: front-side contact occurs when the leading edge of gear 1 meshes with the trailing edge of gear 2, and back-side contact occurs when the trailing edge of gear 1 meshes with the leading edge of gear 2, as shown in Figure 2.

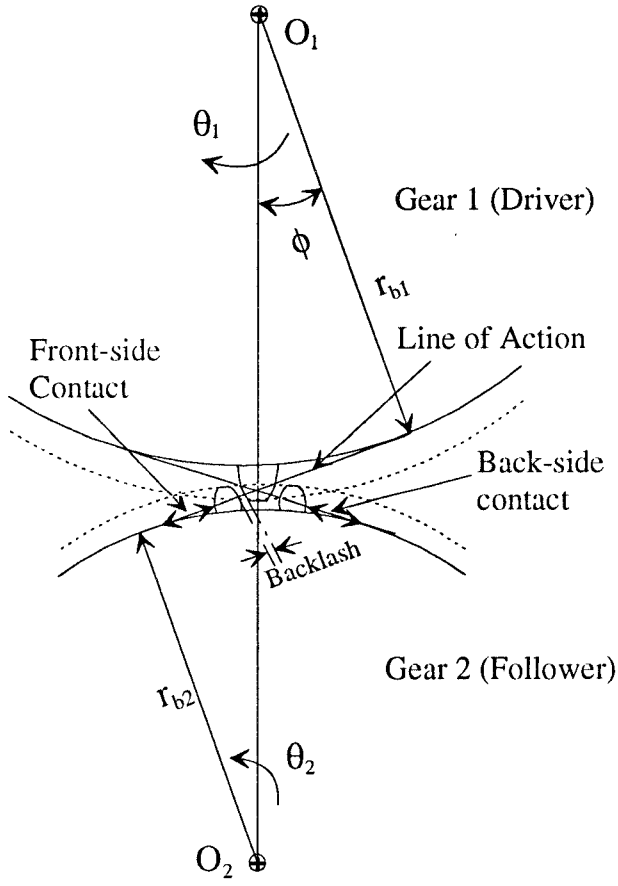

Figure 2: Geometrical relation in meshing gear pair

A modified rotary model for dynamics of spur gear systems with backlash consideration is proposed here. The dynamics of such a system as shown in Figure 2 can be divided into three cases according to whether the two meshing gears are under the front-side contact, separation, or back-side contact. In what follows, we shall neglect the frictional forces at the point of contact and at the journal bearings.

Case(1): Front-side contact

When $r_{b1}\theta_1 - r_{b2}\theta_2 > b$, the leading edge of gear 1 contacts with the trailing edge of gear 2 as shown in Figure 2. The equations of motion can be written as

$$I_1\ddot{\theta}_1 = \xi_1 - F_n r_{b1} \tag{1}$$

$$I_2\ddot{\theta}_2 = \xi_2 + F_n r_{b2} \tag{2}$$

where

$$F_n = k\delta_F + c\dot{\delta}_F \tag{3}$$

and where

$$\delta_F = r_{b1}\theta_1 - r_{b2}\theta_2 - b \tag{4}$$

$$\dot{\delta}_F = r_{b1}\dot{\theta}_1 - r_{b2}\dot{\theta}_2 \tag{5}$$

denote the dynamic transmission error and the relative speed along the line of action, respectively.

Case(2): Separation

When $b > r_{b1}\theta_1 - r_{b2}\theta_2 > -b$, separation occurs and there is no force of interaction between the two gears. Therefore the equations of motion are given by

$$I_1\ddot{\theta}_1 = \xi_1 \tag{6}$$

$$I_2\ddot{\theta}_2 = \xi_2 \tag{7}$$

Case(3): Back-side contact

When $r_{b1}\theta_1 - r_{b2}\theta_2 < -b$, the trailing edge of gear 1 meshes with the leading edge of gear 2. The equations of motion are given by

$$I_1\ddot{\theta}_1 = \xi_1 + F_n r_{b1} \tag{8}$$

$$I_2\ddot{\theta}_2 = \xi_2 - F_n r_{b2} \tag{9}$$

where

$$F_n = k\delta_B + c\dot{\delta}_B \tag{10}$$

and where

$$\delta_B = r_{b2}\theta_2 - r_{b1}\theta_1 - b \tag{11}$$

$$\dot{\delta}_B = r_{b2}\dot{\theta}_2 - r_{b1}\dot{\theta}_1 \tag{12}$$

are the dynamic transmission error and the relative speed along the line of action, respectively. The stiffness function, k, and the damping coefficient, c, will be discussed in following sections.

3 Stiffness Constant Estimation

Yang and Sun (1985) developed a rotary model for the dynamic analysis of a spur gear system with backlash. They also proposed an analytic method to estimate the mesh stiffness constant. In the Yang and Sun's model, they only considered the Hertzian compression, which is a local effect. The effects of bending moment, shear stress, etc. in a gear tooth are not considered. In what follows, the approach proposed by Nakada and Utagawa (1956) will be used with some modifications.

A gear tooth is modeled as a very short cantilever beam with the consideration of some other effects. The cantilever beam consists of two parts: the part inside the base circle is modeled as a rectangular beam and the part outside the base circle is modeled as a trapezoidal beam, as shown in Figure 3. In addition to the deflection contributed by bending moment and shear stress, foundation deflection and Hertzian contact also contribute to the total deflection. That is the overall deflection is expressed as

$$\delta_t = \delta_b + \delta_s + \delta_f + \delta_h \tag{13}$$

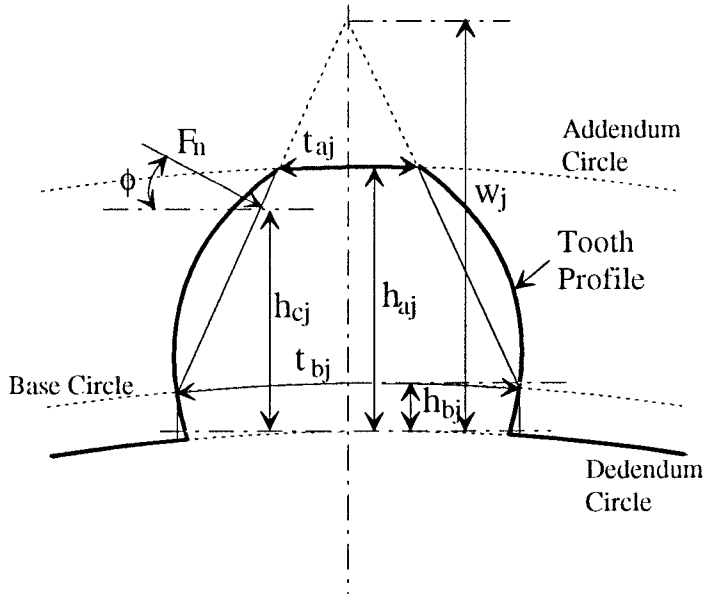

Figure 3: Gear tooth deflection model.

Nakada and Utagawa only considered the bending caused by the tensile force, $F_n \cos\phi$. In the improved model, bending caused by the compressive force, $F_n \sin\phi$, will be also included. Also

the Hertzian deflection derived by Yang and Sun will be included. The various components of deflection for gear j are given as follows (Nakada and Utagawa, 1956; Yang and Sun, 1985):

$$\delta_{bpj} = \frac{12F_n\cos\phi^2 h_{bj}}{Eft_{bj}^3}(h_{cj}^2 + h_{bj}^2/3 - h_{cj}h_{bj}) + \frac{6F_n\cos\phi^2(w_j - h_{bj})^3}{Eft_{bj}^3}$$
$$\times[\frac{w_j - h_{cj}}{w_j - h_{bj}}(4 - \frac{w_j - h_{cj}}{w_j - h_{bj}}) - 2\ln\frac{w_j - h_{cj}}{w_j - h_{bj}} - 3] \quad (14)$$

$$\delta_{bnj} = \frac{3F_n\cos\phi\sin\phi}{Eft_{bj}^2}[\frac{h_{bj}(h_{bj} - 2h_{cj})(w_j - h_{cj})}{w_j - h_{bj}} - (h_{cj} - h_{bj})^2] \quad (15)$$

$$\delta_{sj} = \frac{1.2F_n\cos\phi^2}{Gft_{bj}}[h_{bj} + (w_j - h_{bj})\ln\frac{w_j - h_{bj}}{w_j - h_{cj}}] \quad (16)$$

$$\delta_{fj} = \frac{24F_n\cos\phi^2 h_{cj}^2}{\pi Eft_{bj}^2} \quad (17)$$

$$\delta_{hj} = \frac{4F_n(1-\nu^2)}{\pi Ef} \quad (18)$$

where w_j denotes the height of the triangle shown in Figure 3, and

$$w_j = \frac{h_{aj}t_{bj} - h_{bj}t_{aj}}{t_{bj} - t_{aj}} \quad (19)$$

Therefore the mesh stiffness constant of a tooth on gear j can be denoted as

$$k_j = \frac{F_n}{\delta_{tj}} \quad (20)$$

3.1 Stiffness Constant of a Meshing Gear Pair

Most gear pairs have double-tooth contact, which has an influence on the mesh stiffness function. Hence, some definitions for double-tooth contact will be made. Let AB be the line of action for gears 1 and 2 as shown in Figure 4. Also let line AB be tangent to the base circle of gear 1 at A and that of gear 2 at B and let l be equal to the length of AB. There are four zones along the line of action AB due to the change of the number of pairs of teeth in contact. As shown in Figure 4, point C is the intersection of the addendum circle of gear 2 with line AB, point P is the pitch point, point D is the intersection of the addendum circle of gear 1 with line AB, E and F are two points on AB such that DE=CF=p_b. Sections EP and PF are the single-tooth contact zones and sections CE and FD are the multi-tooth contact zones. The geometric relation between these four zones are

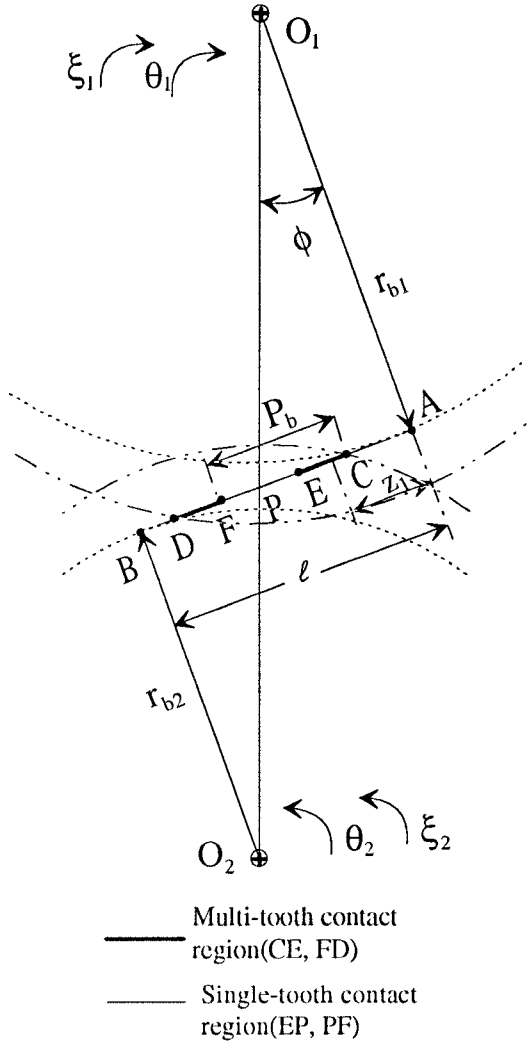

Figure 4: Two-tooth contact

given by

$$\begin{aligned} AB &= l = (r_{b1} + r_{b2}) \tan \phi \\ AC &= l - \sqrt{r_{a2}^2 - r_{b2}^2} \\ AD &= \sqrt{r_{a1}^2 - r_{b1}^2} \\ AE &= AD - p_b \\ AF &= AC + p_b \end{aligned}$$

When two gears are meshing, the two meshing teeth act like two springs in series. When there are two teeth pairs in contact, they act like two springs in parallel. Therefore, the stiffness constant during each mesh cycle can be written as

$$K = \begin{cases} \dfrac{k_{11}k_{21}}{k_{11}+k_{21}} + \dfrac{k_{12}k_{22}}{k_{12}+k_{22}}, & \textit{provided z falls in the double-tooth contact zone} \\ \dfrac{k_{11}k_{21}}{k_{11}+k_{21}} & \textit{provided z falls in the single-tooth contact zone} \end{cases} \tag{21}$$

In what follows, the geometric relations among the parameters used in Equations (14) through (20) will be derived. From the gear tooth definitions, we have

$$h_{bj} = r_{bj} - r_{dj} \tag{22}$$

$$h_{aj} = r_{aj} - r_{dj} \tag{23}$$

However, if the radius of dedendum circle is greater than that of the base circle, then h_{bj} and h_{aj} will be computed as follows:

$$h_{bj} = 0 \tag{24}$$

$$h_{aj} = r_{aj} - r_{bj} \tag{25}$$

From the property of involute gear, as shown in Figure 5, tooth thickness at a general location can be written as (Steeds, 1948)

$$t_m = r_m[\frac{t_p}{r_p} + 2(inv\phi_p - inv\phi_m)] \tag{26}$$

where $r_p = (r_b)/(\cos\phi)$, $r_m = (r_b)/(\cos\phi_m)$ is the radius at meshing point M, *inv* is the involute

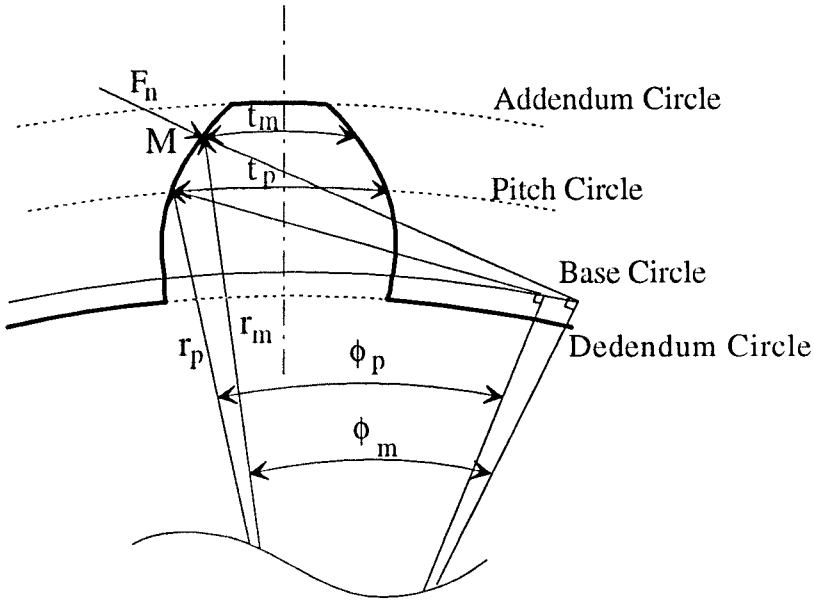

Figure 5: Tooth Thickness.

function such that $inv\,\phi = \tan\phi - \phi$. Therefore the tooth thickness at base circle of gear j, t_{bj}, is given by

$$t_{bj} = r_{bj}[\frac{t_p}{r_{pj}} + 2(\tan\phi - \phi)] \tag{27}$$

Similarly, the tooth thickness along addendum circle of gear j, t_{aj}, is given by

$$t_{aj} = r_{aj}[\frac{t_p}{r_{pj}} + 2(inv\phi - inv\beta_j)] \tag{28}$$

where $\beta_j = \cos^{-1}(r_{bj}/r_{aj})$.

Due to the property of involute gear tooth, the relation between the rotation angle measured from O_1A, α_{ij}, and the operating pressure angle on gear teeth at point M, ϕ_m, as shown in Figure 6, is given by

$$\alpha_{ij} = \tan\phi_m \tag{29}$$

Therefore referring to Figure 6, γ_m and h_{cj} are given by

$$\gamma_m = \frac{t_m}{2r_m} = 0.5[\frac{t_p}{r_p} + 2(inv\phi - inv\phi_m)] \tag{30}$$

$$\begin{aligned} h_{cj} &= r_{mj} - r_{dj} = \frac{r_{bj}\cos\gamma_m}{\cos\phi_m} - r_{bj} + h_{bj} \\ &= [\frac{\cos\gamma_m}{\cos(\tan^{-1}\alpha_{ij})} - 1]r_{bj} + h_{bj} \end{aligned} \tag{31}$$

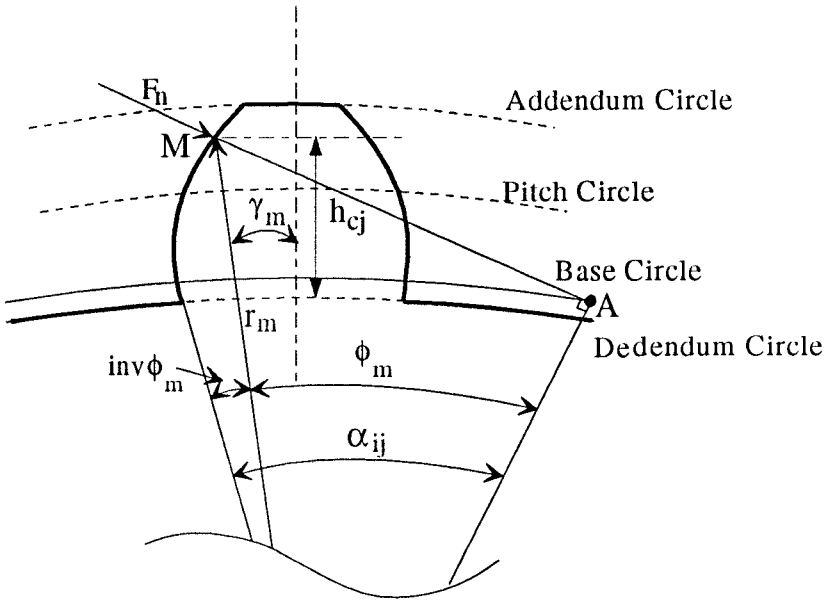

Figure 6: Tooth length and angle relations.

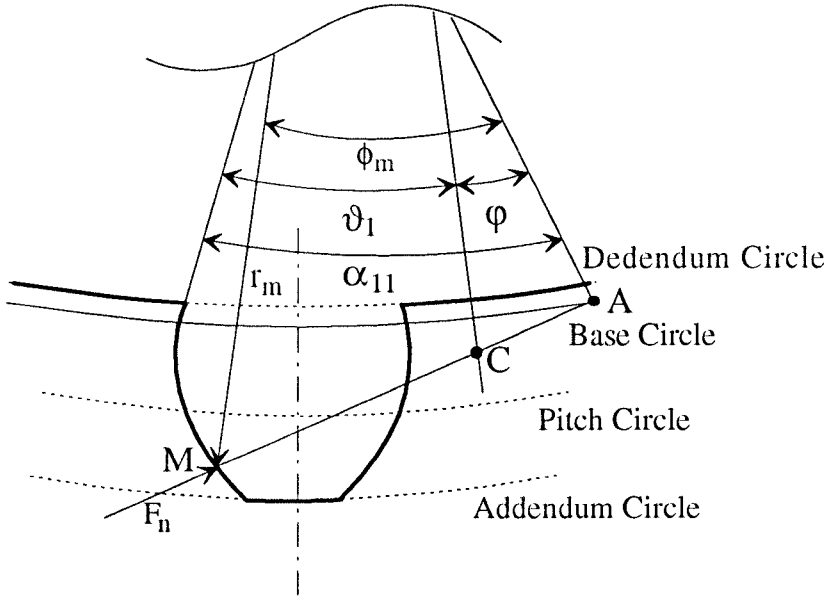

Figure 7: Relations between angles, α_{11}, φ, ϕ_m, and ϑ_1.

Note that h_{aj}, h_{bj}, t_{aj} and t_{bj} are constants while h_{cj} and t_m are function of α_{ij}. Since the first contact point C is decided by the addendum circle of the mating gear, there exists an offset angle, φ, between O_jA and O_jC. The offset angle for gear 1, for example, is equal to $(AC)/(r_{b1})$ as shown in Figure 7. Hence the relations between the rotation angle of the first meshing gear teeth of gear 1, denoted as α_{11}, and of gear 2, denoted as α_{21}, are given by

$$\alpha_{11} = \vartheta_1 + \frac{AC}{r_{b1}} \tag{32}$$

$$\alpha_{21} = \frac{(l - \alpha_{11} r_{b1})}{r_{b2}} \tag{33}$$

where ϑ_1 is the rotation angle measured from the line O_1C to O_1M.

The corresponding rotation angles of the second meshing gear teeth, denoted as α_{12} and α_{22}, are

$$\alpha_{12} = \alpha_{11} + \frac{p_b}{r_{b1}} \tag{34}$$

$$\alpha_{22} = \alpha_{21} - \frac{p_b}{r_{b2}} \tag{35}$$

Equations (34) and (35) is valid only when α_{11} is in approach section.

Substituting Equations (32)–(35) into Equation (31), h_{cj} can be calculated at very instant of rotation. Substituting the values of h_{aj}, h_{bj}, h_{cj}, t_{aj}, t_{bj}, and t_{mj} into Equations (14)–(18) and the resulting values into Equation (20), the stiffness constant of a single tooth can be found. Substituting the stiffness constants of all the meshing teeth into Equation (21), the overall mesh stiffness constant can be evaluated. Note that a gear pair will make a complete cycle of meshing when a pair of teeth starts their meshing at point C and ends at point F.

3.2 Example

Two gears are chosen to illustrate the principle. The gear parameters are taken from Yang and Sun (1985). They are listed as follows: density for steel, ρ=7800 kg/m^3; Young's modulus, $E_1 = E_2 = 2.068e11\ N/m^2$; Poisson's ratio, $\nu_1 = \nu_2 = 0.3$; pitch radii for gears 1 and 2, $r_1 = 0.02\ m$ and $r_2 = 0.08\ m$; pressure angle, $\phi = 20\ deg$; number of teeth, $N_1 = 20$ and $N_2 = 80$; face width, $f = 0.01\ m$; backlash, $b = 0.00005\ m$; damping ratio, $\zeta = 0.05$. From the above data, the moments of inertia of gears 1 and 2 are computed as $I_1 = 1.9604e-05\ kg \cdot m^2$ and $I_2 = 0.0050\ kg \cdot m^2$,

respectively. From the above data, it can be proven that the contact ratio is equal to 1.69129, i.e., this is a double-tooth contact pair.

First, all components of deflection produced by a unit load, $1N$, at gears 1 and 2 are calculated and plotted as functions of ϑ_1 as shown in Figures 8 and 9, respectively. It can be seen from

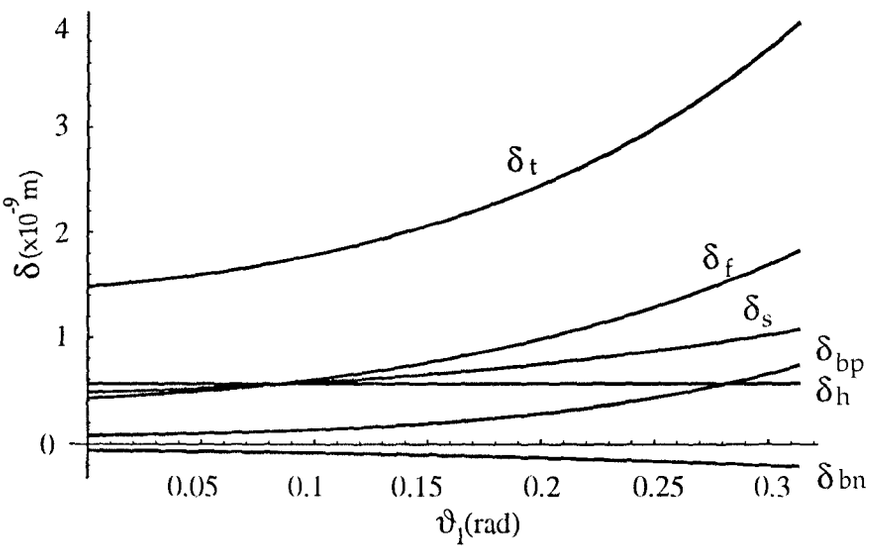

Figure 8: Deflection of gear 1 vs. ϑ_1

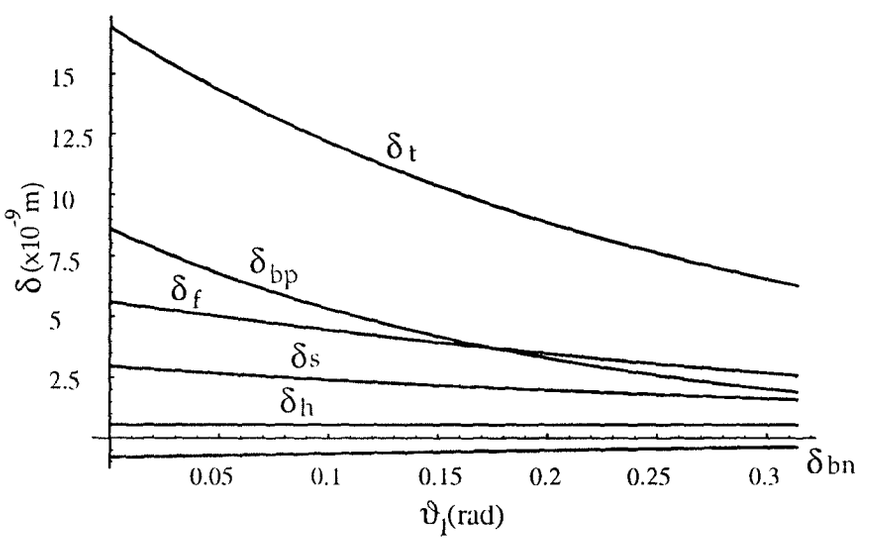

Figure 9: Deflection of gear 2 vs. ϑ_1

Figure 8 that when the contact point is near the base circle, i.e., $\vartheta_1 < 0.1$, the Hertzian compression and the other deflections are all very small. But when the contact point is near the addendum circle, the deflection due to shear, δ_s, and the deformation of tooth foundation, δ_f, become the dominant

terms, while the deflection caused by the negative bending moment, δ_{bn}, is insignificant. Referring to Figure 9, we note that the deflections due to bending moment, shear stress, and foundation deformation are all large when $\vartheta_1 < 0.1$, and the deflections decrease as the contact point moves closer to the base circle. However, the deflections due to Hertzian contact and negative bending moment are always very small. The difference in the contribution of various components shown in Figures 8 and 9 are caused by the difference in the tooth lengths between gears 1 and 2. The resultant stiffness constant k for a single tooth on gears 1 and 2, and their combined stiffness are shown in Figure 10. The combined stiffness is very close to a constant . The stiffness constant of the example gear pair with the consideration of double-tooth contact is shown in Figure 11. As can be seen from Figure 11, the stiffness constant decreases drastically as the mesh changes from a two-tooth contact to a single-tooth contact.

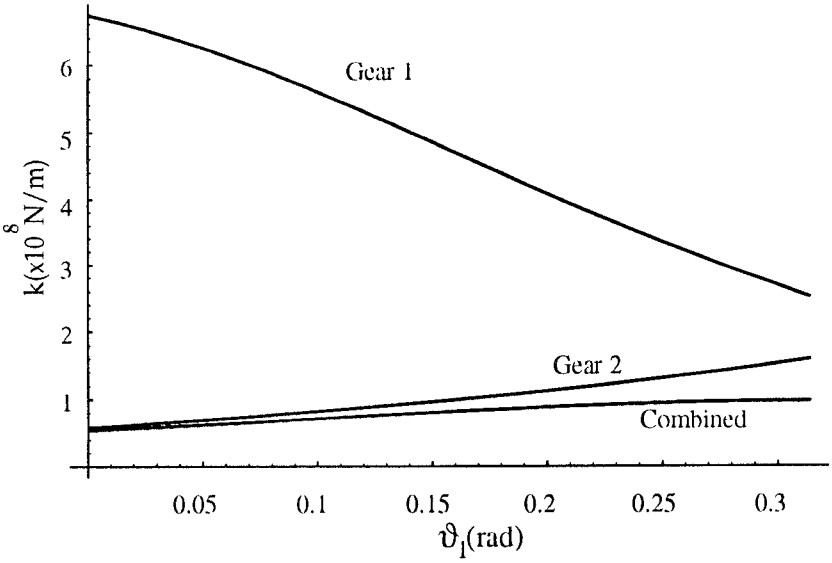

Figure 10: Stiffness constant vs. ϑ_1

Since it is not feasible to keep track of the variation of the mesh stiffness constant k in a real time control system, the mean value of k can be used for control purpose. The mean value and the magnitudes of the first and second harmonics are shown in Table 1, where C_1 denotes the coefficient of the first harmonic and C_2 denotes the coefficient of the second harmonic. We note that the first harmonic and the second harmonic are one order-of-magnitude smaller than the mean value. Using the mean value alone will introduce some error in the model. However, the actual frequency of occurance due to the first harmonic is equal to the product of the number of teeth and the angular

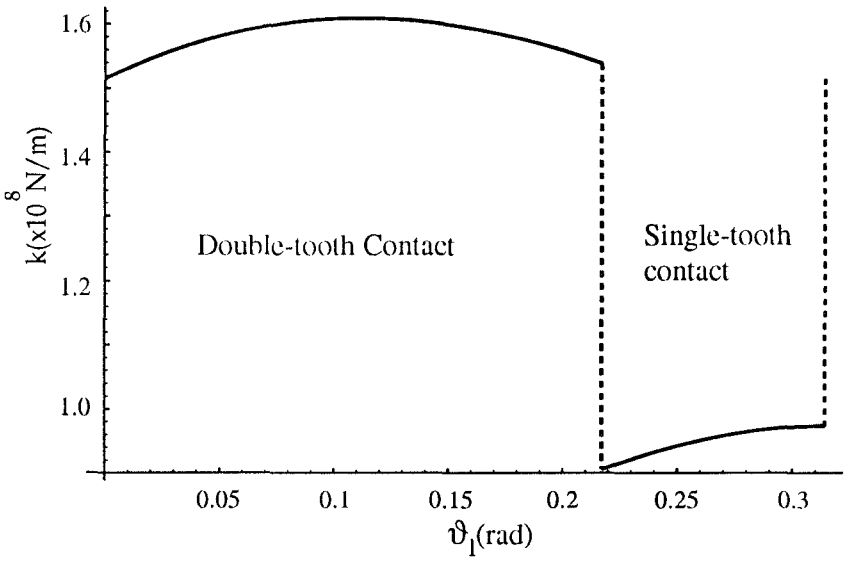

Figure 11: Stiffness constant vs. ϑ_1

	Mean	C_1	C_2
K	$1.3868 \cdot 10^8$	$2.956 \cdot 10^7$	$1.684 \cdot 10^7$

Table 1: Mesh stiffness (N/m)

velocity in revolution per second of the drive gear. This results in a relatively high frequency in comparison with the bandwidth of a mechanical system and, hopefully, will have little effect on the dynamics of a geared servomechanism.

4 Damping constant

Dubowsky and Freudenstein (1971) first created a dynamic model, known as the "Impact Pair," to describe the dynamics of mechanical systems with clearance. But the conventional linear law they used for the normal contact force formula, $c\dot{x} + kx$, results in a non-zero damping force at the time of impact and unrealistic tensile force at the time of separation due to non-zero relative velocity. Hence Azar and Crossley (1977) proposed a nonlinear law for the normal contact force, $(d\dot{x} + k)x$, to avoid this problem. Based on Azar and Crossley's approach, Yang and Sun (1985) developed a circular model for spur gear system with backlash, They also proposed an analytic method to estimate the damping factor of a gear tooth. The formula they used is

$$d = \frac{6(1-e)}{[(2e-1)^2+3]} \cdot \frac{k}{V_i} \tag{36}$$

where V_i is the impact velocities, and e is the coefficient of restitution which can be obtained from

$$e = 1 - 0.022V_i^{0.36} \tag{37}$$

Hence the damping factor, d, used by Yang and Sun, which depends on the impact velocities, V_i, needs to be determined at the instant of impact and is not practical for real time control system. Also, the coefficient of restitution used for calculation of damping factor is obtained from experiment of ball to ball impact (Goldsmith, 1960). The deflection due to bending moment, shear force, etc. are not considered. Its validity for impact between gear teeth may be questionable. Based on the above reasoning, the approach proposed by Dubowsky and Freudenstein (1971), known as the "Impact Pair," is adopted. Although it may cause a little error, it is simpler and has been shown to be more stable (Herbert and McWhannell, 1977). Hence in the improved model, the linear law $k\delta + c\dot{\delta}$ is used to calculate the contact force. Also, the damping coefficient, c is assumed to be time independent and can be determined by experiments. Its relation with the damping ratio, ζ, is given by

$$c = 2\zeta\sqrt{k\frac{I_2 r_{b1}^2 + I_1 r_{b2}^2}{I_2 I_1}} \tag{38}$$

5 Comparison with Yang and Sun's Model

In this section, the difference between Yang and Sun's and our improved model will be discussed and compared. Yang and Sun only considered the meshing stiffness from the Hertzian contact. In this work, the stiffness constant k is an average value taken from the combined effects of bending moment, shear stress, Hertzian contact, foundation inclination and the multi-tooth contact. As a result, the value of k is several times smaller than that used in the Yang and Sun's model. Also, the algorithm used by Yang and Sun in deriving the damping factor are no longer valid since the deflection contributed by Hertzian contact is insignificant in comparison with that due to bending moment, shear force, etc. Assuming a damping ratio of $\zeta = 0.05$, and using the gear data from previous calculations, the damping coefficient for the improved model is calculated from Equation (38) as c=237.6651 $N \cdot s/m$.

5.1 Simulation Results

To compare the difference in dynamic behavior between Yang and Sun's model and the improved model, two types of simulation were performed: free vibration and constant load operation. For convenience, the stiffness and damping functions used in Yang and Sun's model were derived from single-tooth contact model. The stiffness function used in Yang and Sun's model is

$$k = \frac{\pi E f}{4(1-\nu^2)} \tag{39}$$

The damping function used in Yang and Sun's model is as described in Equations (36) and (37).

The software used for simulation is Simulink (MathWorks, Inc., 1992) and the integration method chosen is the Runge-Kutta 5th order method with a fourth order step-size control. This package provides an advantage of flexible integration step size which can reduce the computation time required since the dynamic system under study is a discontinuous and "hard" system. The maximum step size is 1e-4 sec, the minimum step size is 1e-6 sec, and tolerance is set at 1e-6.

5.1.1 Free Vibration

The initial velocities of gears 1 and 2 are chosen to be $\dot{\theta}_1 = 50\ rad/s$ and $\dot{\theta}_2 = 0\ rad/s$, respectively, and the initial positions of both gears are set at their neutral positions as defined in section 2. The simulation results are shown in Figures 12 through 16. Figures 12 through 15 show the angular displacements and angular velocities of both gears wherein the solid line represents the response of Yang and Sun's model and the dashed line is the response of our improved model. The two gears bounce back and forth from front-side contact to rear-side contact which causes the angular displacement to deviate from a straight line. The frequency of deviation from a straight line is different for the two models since the stiffness constants and damping functions used in the two models are different. But the basic trend is similar. The deviation of the angular displacement of gear 2 from a straight line is much smaller than that of gear 1 due to the larger moment of inertia of gear 2 and the gear ratio. The average angular velocities of both gears are both positive, but the instantaneous velocity of gear 1 sometimes becomes negative. There exists periods of constant angular velocities for both gears 1 and 2, which correspond to the periods of separations between the two gears. The relative displacements are shown in Figure 16. Since the damping factor used in the Yang and Sun's model increases as a function of time, the frequency of vibration will also

change as a function of time as can be seen from Figure 16. Before 4 ms, the frequency of Yang and Sun's model is lower than, but after that it becomes higher than that of the improved model. The successive impacts can be clearly seen from Figure 16 as s becomes greater than 0.05 mm or less than -0.05 mm. Also due to the greater stiffness constant used in the Yang and Sun's model, the penetration, i.e., $|s|$-0.05 mm obtained from the Yang and Sun's model is also smaller than that of the improved model.

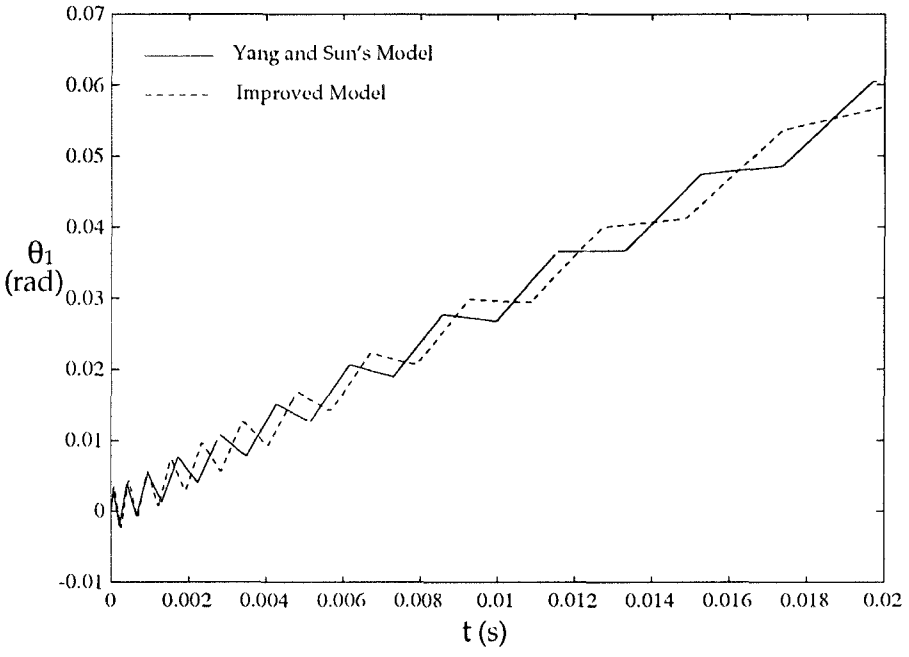

Figure 12: Angular displacement of gear 1 under free vibration

5.1.2 Constant Load Operation

The initial velocities of gears 1 and 2 are chosen to be $\dot{\theta}_1 = 50\ rad/s$ and $\dot{\theta}_2 = 0\ rad/s$, respectively, and the initial positions of both gears are set at their neutral positions. A constant torque of ξ_1=1 Nm is applied on gear 1 and an equal but opposite sign load, ξ_2=1 Nm, is applied on gear 2. The simulation results obtained from the two models are shown in Figures 17 through 21. Figures 17 through 20 show the angular displacements and angular velocities of both gears. The relative displacements are shown in Figure 21. The angular displacements obtained from both models are almost identical. The angular velocities of both gears deviate from a straight line because of the impacts between the two gears. Due to larger stiffness constant used in the Yang and

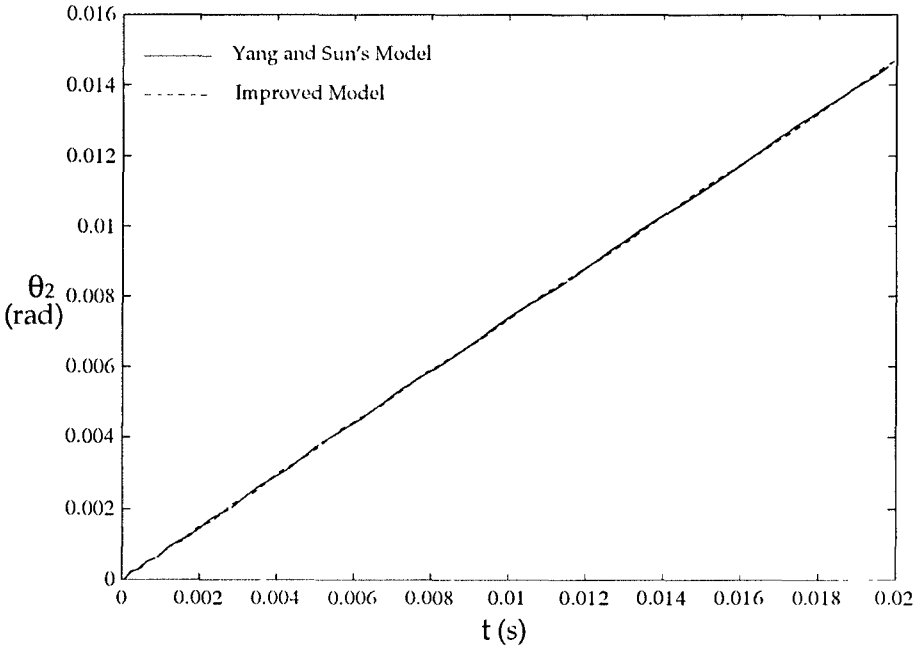

Figure 13: Angular displacement of gear 2 under free vibration

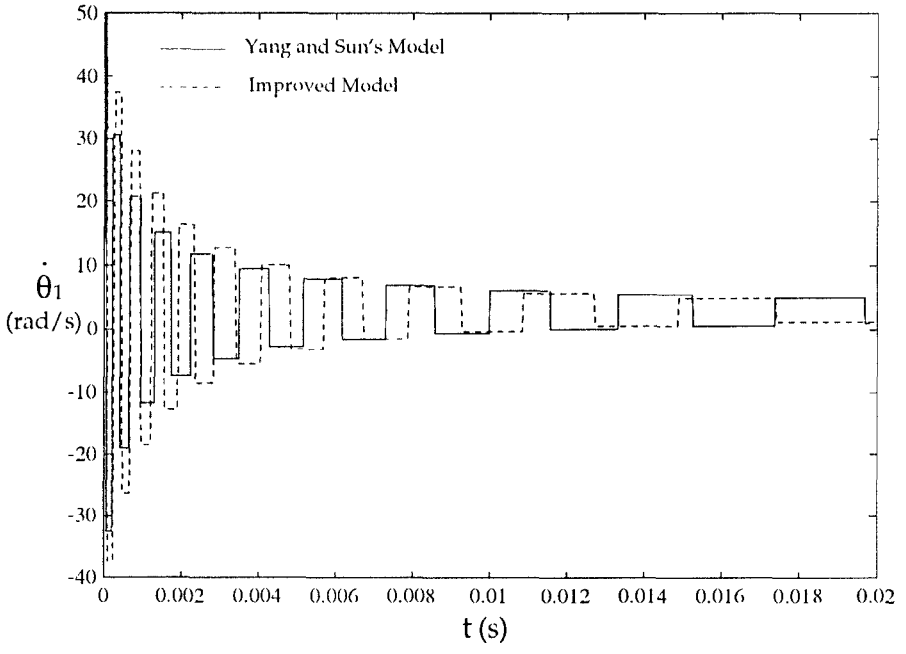

Figure 14: Angular velocity of gear 1 under free vibration

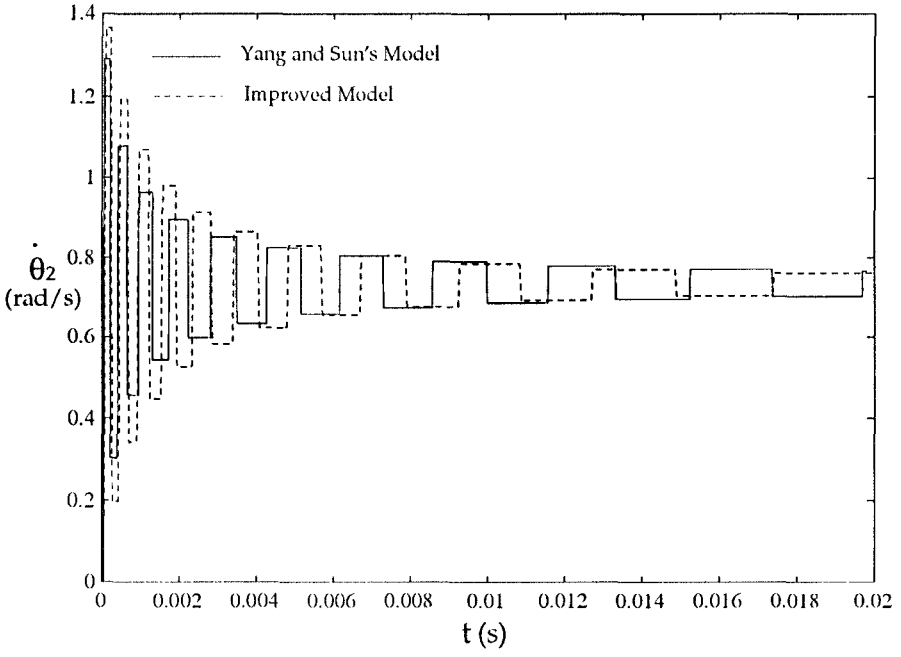

Figure 15: Angular velocity of gear 2 under free vibration

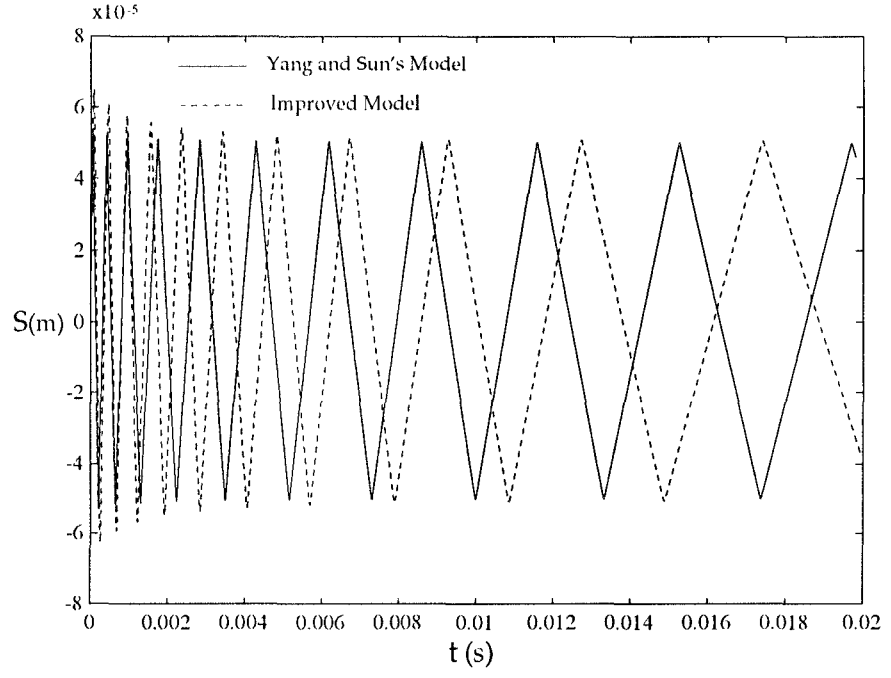

Figure 16: Relative displacement under free vibration

Sun's model, the amplitude of oscillations in angular velocity is also smaller. From Figure 21, we observe that the successive impacts initially occurs on both sides of a gear tooth and then changes to one side contact.

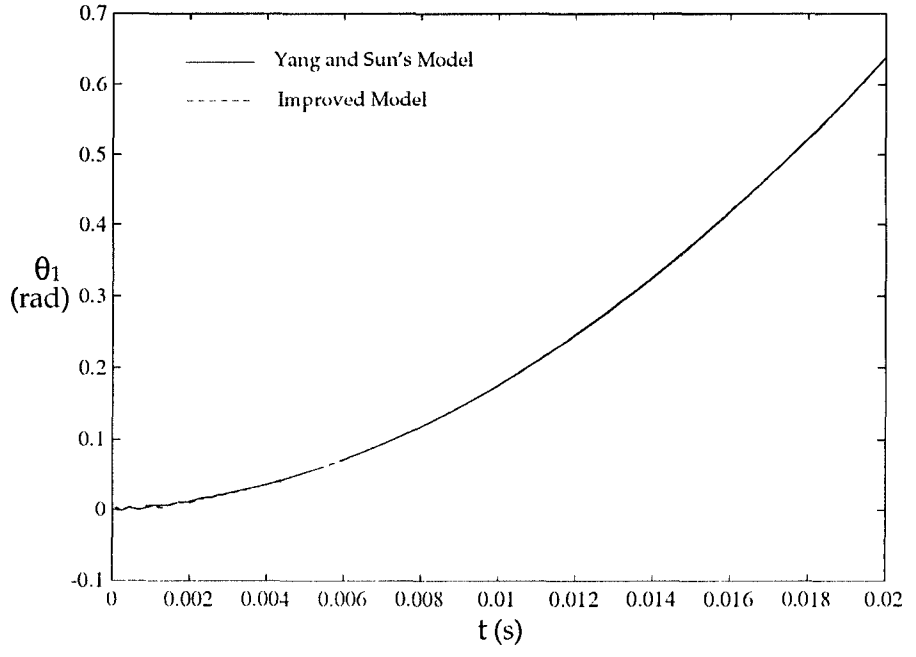

Figure 17: Angular displacement of gear 1 under constant load

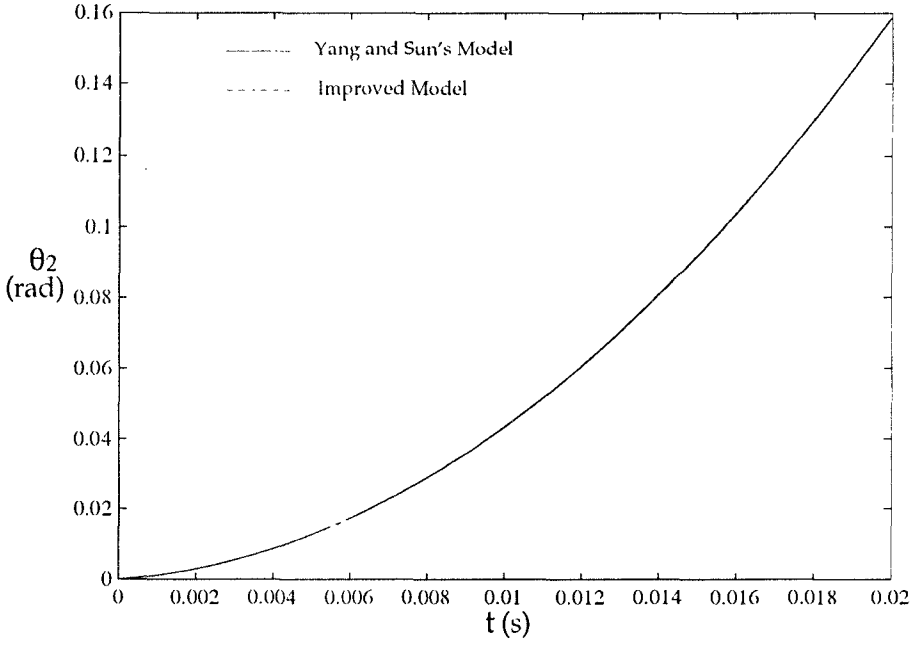

Figure 18: Angular displacement of gear 2 under constant load

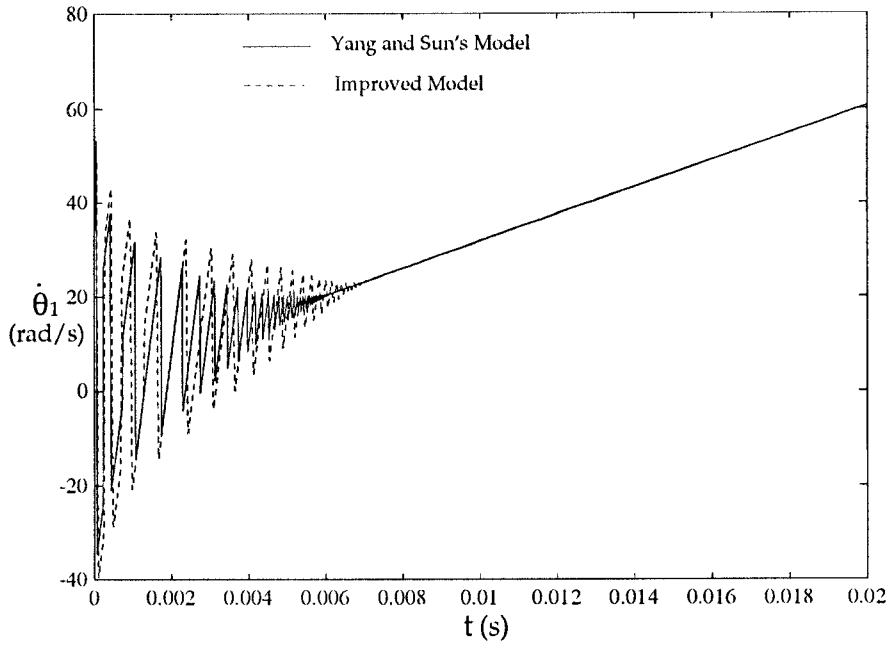

Figure 19: Angular velocity of gear 1 under constant load

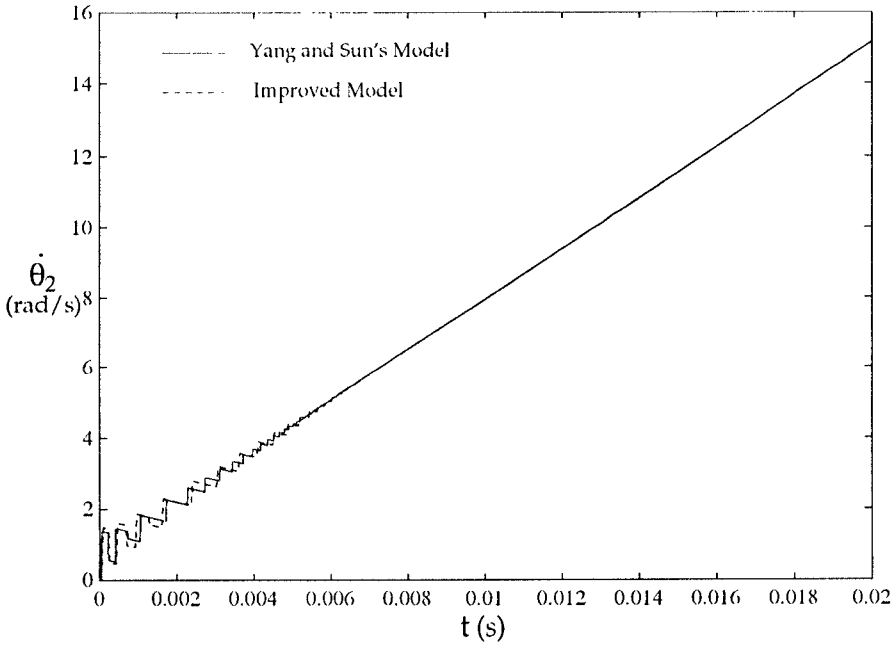

Figure 20: Angular velocity of gear 2 under constant load

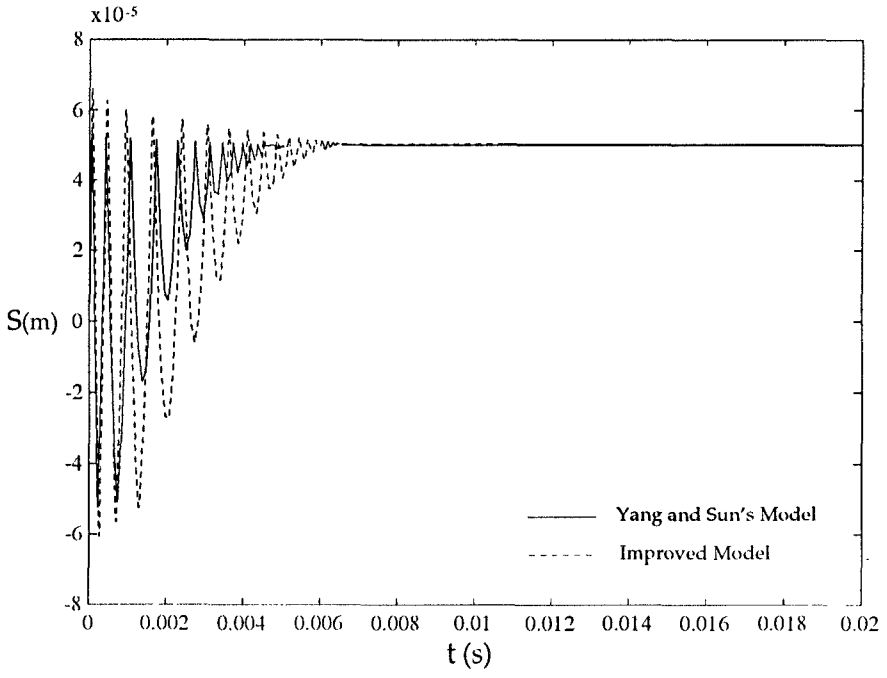

Figure 21: Relative displacement under constant load

6 Conclusions

An improved dynamic model which considers the effects of backlash in a spur gear system for the purpose of precision control has been proposed. Equations for evaluation of the mesh stiffness were derived. Two simulations were performed to illustrate the effects of backlash on the dynamics of a typical gear pair. The first is a free vibration and the second is a constant load operation. Both the Yang and Sun's model and the improved model were used for the simulations. It can be concluded from the comparison study that the improved model is much simpler, it does not require online estimation of the stiffness constant and damping coefficient, and meanwhile improves the accuracy of the model. Hence, the improved model is more suitable for real time control.

Acknowledgment

This work was supported by the NSF Engineering Research Centers Program, NSFD CDR 8803012. Such support does not constitute an endorsement of the views expressed in the paper.

References

Azar, R. C. and Corssley, F. R. E., 1977, "Digital Simulation of Impact Phenomenon in Spur Gear Systems," ASME Journal of Engineering for Industry, pp. 792–798.

Comparin, R. J. and Singh, R., 1989, "Nonlinear Frequency Response Characteristics of an Impact Pair," Journal of Sound and Vibration, Vol. 134, No. 2, pp. 259–290.

Dubowsky, S. and Freudenstein, F., 1971, "Dynamic Analysis of Mechanical Systems with Clearance Part 1 and 2," ASME Journal of Engineering for Industry, pp. 305–316.

Elkholy, A. H., 1985, "Tooth Load Sharing in High-Contact Ratio Spur Gears," ASME Journal of Mechanisms, Transmissions, and Automation in Design, Vol. 107, pp. 11–16.

Goldsmith, W., 1960, *Impact: The Theory and Physical Behavior of Colliding Solids*. Edward Arnold, London.

Goodman, T. P., 1963, "How to Calculate Dynamic Effects of Backlash," Machine Design, pp. 150–157.

Herbert, R. G. and McWhannell, D. C., 1977, "Shape and Frequency Composition of Pulses From an Impact Pair," ASME Journal of Engineering for Industry, pp. 513–518.

Hunt, K. H. and Crossley, F. R. E., 1975, "Coefficient of Restitution Interpreted as Damping in Vibroimpact," ASME Journal of Applied Mechanics, pp. 440–445.

Kahraman, A. and Singh, R., 1989, "Nonlinear Dynamics of a Spur Gear Pair," Journal of Sound and Vibration, pp. 49–75.

Lee, T. W. and Wang, A. C., 1983, "On the Dynamics of Intermittent Motion Mechanisms, Part 1," ASME Journal of Mechanisms, Transmissions, and Automation in Design, Vol. 105, pp. 534–540.

Martin, G. H., 1982, *Kinematics and Dynamics of Machines*. McGraw-Hill, New York.

MathWorks, Inc., 1992, *Simulink User's Guide*. Natick, Massachusetts.

Matsuz, J. M., O'donnell, W. J., and Erdlac, R. J., 1969, "Local Flexibility Coefficients for the Built-In Ends of Beams and Plates," ASME Journal of Engineering for Industry, pp. 607–614.

Nakada, T. and Utagawa, M., 1956, "The Dynamic Loads on Gear Caused by the Varying Elasticity of the Mating Teeth," *Proceedings of the 6th Japan National Congress for Applied Mechanics*, pp. 493–497.

O'Donnel, W. J., 1960, "The Additional Deflection of a Cantilever Due to the Elasticity of the Support," ASME Journal of Applied Mechanics, pp. 461–464.

Ozguven, H. N. and Houser, D. R., 1988, "Mathematical Models Used in Gear Dynamics- A Review," Journal of Sound and Vibration, Vol. 121, No. 3, pp. 383–411.

Rebbechi, B. and Crisp, J., 1981, "A New Formulation of Spur-Gear Vibration," *International Symposium on Gearing and Power Transmission*, pp. 61–66.

Remmers, E. P., 1971, "The Dynamics of Gear Pair systems," *71-DE-23*.

Steeds, W., 1948, *Involute Gears*. Longmans, Green & CO., New York.

Tavakoli, M. S. and Houser, D. R., 1986, "Optimum Profile Modifications for the Minimization of Static Transmission Errors of Spur Gears," ASME Journal of Mechanisms, Transmissions, and Automation in Design, Vol. 108, pp. 86–94.

Timoshenko, S. and Baud, R. V., 1926, "The Strength of Gear Teeth," Mechanical Engineering, Vol. 48, No. 11, pp. 1105–1109.

Tobe, T. and Takatsu, N., 1973, "Dynamic Loads on Spur Gear Teeth Caused by Teeth Impact," Bulletin of JSME, Vol. 16, No. 96, pp. 1031–1037.

Yang, D. C. H. and Sun, Z. S., 1985, "A Rotary Model for Spur Gear Dynamics," ASME Journal of Mechanisms, Transmissions, and Automation in Design, Vol. 107, pp. 529–535.